ACS Sustainable Chemistry & Engineering

Research Article

Cite This: ACS Sustainable Chem. Eng. 2018, 6, 14847−14856

pubs.acs.org/journal/ascecg

Copper Based Nanomaterials Suppress Root Fungal Disease in Watermelon (*Citrullus lanatus*): Role of Particle Morphology, Composition and Dissolution Behavior

Jaya Borgatta,[†] Chuanxin Ma,[†] Natalie Hudson-Smith,[‡] Wade Elmer,[§] Cristian David Plaza Pérez,[§,⊥] Roberto De La Torre-Roche,[∥] Nubia Zuverza-Mena,[∥] Christy L. Haynes,[‡] Jason C. White,*[,∥] and Robert J. Hamers*[,†]

[†]Center for Sustainable Nanotechnology, Department of Chemistry, University of Wisconsin−Madison, 1101 University Avenue, Madison, Wisconsin 53706, United States

[‡]Center for Sustainable Nanotechnology, Department of Chemistry, University of Minnesota, 207 Pleasant Street S.E., Minneapolis, Minnesota 55455, United States

[§]Department of Plant Pathology and Ecology, The Connecticut Agricultural Experiment Station, 123 Huntington Street, New Haven, Connecticut 06504, United States

[⊥]Department of Fitopatologia, Federal University of Lavras, Lavras 37200-000, Brazil

[∥]Department of Analytical Chemistry, The Connecticut Agricultural Experiment Station, 123 Huntington Street, New Haven, Connecticut 06504, United States

Supporting Information

ABSTRACT: With increasing global population, innovations in agriculture will be essential for a sustainable food supply. We compare commercial CuO NP to synthesized $Cu_3(PO_4)_2{\cdot}3H_2O$ nanosheets to determine the influence of coordinating anion, particle morphology, and dissolution profile on *Fusarium oxysporum* f. sp. *niveum* induced disease in watermelon. Copper dissolution in organic acid solutions that mimic complexing agents found in plants was increased by 2 orders of magnitude relative to water. $Cu_3(PO_4)_2{\cdot}3H_2O$ nanosheets showed a rapid initial dissolution, with equilibration after 24 h; CuO NP exhibited continuous particle dissolution. In a greenhouse study, $Cu_3(PO_4)_2{\cdot}3H_2O$ nanosheets at 10 mg/L significantly repressed fungal disease as measured by yield and by a 58% decrease in disease progress. Conversely, CuO NP only yielded significant effects on disease at 1000 mg/L. In field studies, similar enhanced disease suppression was noted for $Cu_3(PO_4)_2{\cdot}3H_2O$ nanosheets, although biomass and yield effects were variable. The method of application was a significant factor in treatment success, with the dip method being more effective than foliar spray; this is likely due to homogeneity of coverage during treatment. The data show that Cu-based nanoscale materials can be an effective and sustainable strategy in the crop disease management but that particle characteristics such as morphology, coordination environment, and dissolution profile will be important determinants of success.

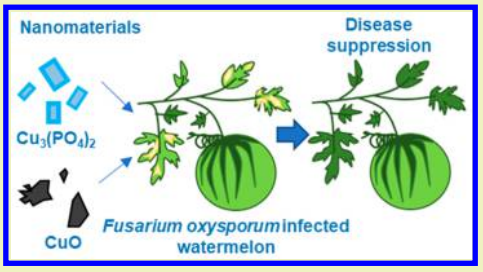

KEYWORDS: *Copper phosphate nanosheets, Watermelon, Fusarium oxysporum f. sp. niveum, Foliar application, Disease suppression*

INTRODUCTION

As the global population continues to grow toward 9.7 billion by 2050,[1] new agricultural production strategies must be explored to achieve sustainable food security, especially as water and arable land become more limited resources.[2] A number of innovations in agricultural practices and chemical additives, described here as amendments, have been proposed to increase crop yields with minimal additional input of resources. These practices include using sensors to monitor crop quality, prescriptive planting, genetic modification, and the development of new agrichemical delivery systems.[3−5] Crop losses from disease and pests remain a significant problem, leading to 20−40% decreases in yield and subsequent economic losses, thus threatening overall food security.[6] One area of active focus has been on micronutrients, which are known to be critical to plant response against disease by acting as enzyme cofactors to promote the formation of defensive secondary metabolites.[7] However, micronutrient availability in soil is often low due to either alkaline conditions or complexation with organic matter.[8,9] In addition, translocation from leaves to roots is restricted for many nutrients, meaning that foliar applications are largely ineffective for root pathogens such as fungi and nematodes. Nanomaterials have been proposed as a more effective micronutrient delivery system

Received: July 15, 2018
Revised: August 30, 2018
Published: October 2, 2018

DOI: 10.1021/acssuschemeng.8b03379
ACS Sustainable Chem. Eng. 2018, 6, 14847−14856

than traditional methods due to their high surface area and reactivity, as well as potential enhanced transport within plant tissues.[3] Furthermore, there is great interest in tuning material characteristics to customize micronutrient release for optimum success.[3,8,10]

There have been several recent investigations on the use of copper nanomaterials based on the known antimicrobial and antifungal properties of the metal ions.[4,11−14] Traditionally, copper has been applied to crops in either salt or bulk hydroxide form for pathogen control.[15,16] Although somewhat effective for the intended purpose, this application of solubilized copper salts can lead to the accumulation of copper in the field, as well as leaching to fresh water sources.[17] The long-term influence of copper accumulation on the soil microbiome and on aquatic species, as well as potential hazards to human health, are not known.[8,18,19] To efficiently supply plants with antifungal copper, several strategies based on different nanomaterials have been explored, including CuO, CuS and $Cu(OH)_2$, and even commercially available products such as Kocide (approximately 46% copper hydroxide particles ranging in size from nanoparticles to micrometer sized particles).[10,12,14,20−22] These materials have been shown to reduce disease incidence at lower concentrations than required using soluble salts. For example, a previous study reported that tomato bacterial spot was reduced using Cu composite nanomaterials at Cu concentrations nearly 10-fold lower than the concentration of commercial Kocide or Cu Mancozeb. Similarly, nanomaterials have been found to reduce disease in cucumber and citrus plants.[4,23] While it is possible that the nanomaterial interact directly with the plant system, several researchers have suggested that the mode of action of copper-based nanomaterials is due to the enhanced release of ions, more effectively stimulating the plant defenses and promoting the formation of secondary metabolites.[23,24] Furthermore, copper amendments under certain treatment regimens may directly reduce bacterial and fungal growth.[12,20,25,26] In spite of the obvious importance of particle dissolution, little research has been directed at the controlled release of copper ions from nanomaterials for agricultural applications.

Traditionally, metal phosphates have been used as inorganic coatings to tune the release of ions through the generation of insoluble solids.[27] Phosphate in the form of buffered phosphate solutions, phosphorous acid salts, or organic-phosphate compounds has shown the reduction of bacterial and fungal infections. In addition, there was enhanced antimicrobial activity when phosphate compounds were applied concurrently with solubilized copper salts.[4,28,29] In a previous study, researchers synthesized nanostructured copper phosphate protein composites that showed antifungal properties *in vitro*.[12,30−35] However, the application of copper phosphate nanomaterials to suppress disease and enhance crop yield remains largely unexplored.

In this paper, we investigate the use of $Cu_3(PO_4)_2{\cdot}3H_2O$ nanosheets, commercially available CuO nanoparticles (NP) and $CuSO_4$ solution (consisting of free Cu^{2+} and SO_4^{2-} ions) as amendments on watermelon to improve resistance to the soilborne fungus *Fusarium oxysporum* f. sp. *niveum* and to increase yield. In two separate greenhouse experiments, different application strategies (foliar spray and foliar dip) and a broad range of amendment concentrations were investigated to gain a better mechanistic understanding of disease suppression and yield enhancement potential. In addition, field experiments at two different farm locations were conducted to assess if observed successful results in the greenhouse translate to a field application. The findings of this study demonstrate that aqueous suspensions of $Cu_3(PO_4)_2{\cdot}3H_2O$ nanosheets are more effective than suspensions of commercial CuO nanoparticles and aqueous solutions of $CuSO_4$ at reducing fungal disease, while also increasing total wet mass, an important measure of plan growth. These results suggest that nanoparticle composition, nanoparticle shape and the associated differences in Cu^{2+} release rate may be important factors controlling the beneficial agricultural effects of nanomaterials.

MATERIALS AND METHODS

Materials and Synthesis. CuO nanoparticles (30 nm diameter; powder) were obtained from U.S. Research Nanomaterials (Houston TX). Copper chloride dihydrate, ammonium phosphate monobasic and diethylene glycol were obtained from Sigma-Aldrich (St. Louis MO). All reagents were used without further purification. We synthesized $Cu_3(PO_4)_2{\cdot}3H_2O$ nanosheets using a polyol method.[36,37] Nanoparticles of $Cu_3(PO_4)_2{\cdot}3H_2O$ form in a two-dimensionally sheet-like morphology; we refer to these as "nanosheets". First, 4 mL of 2 M $CuCl_2{\cdot}2H_2O$ was added to 20 mL of diethylene glycol, and the mixture was heated to 140 °C under reflux for an hour. A 4 mL aliquot of 1.3 M solution of $NH_4H_2PO_4$ was then rapidly injected into the reaction mixture, and the reaction proceeded for 5 h. The nanosheets were then isolated by centrifugation at 5000 rpm using a Thermo Fischer Sorvall Legend X1R centrifuge and were then rinsed with ethanol (2×) and water (1×), followed by drying overnight under vacuum. For all reported experiments, the mass concentration expressed as mg/L of nanoscale CuO and $Cu_3(PO_4)_2{\cdot}3H_2O$ materials were used. However, through ICP-OES we determined the elemental Cu contribution (described below) in CuO nanopartcles is 85 ± 6%, whereas for $Cu_3(PO_4)_2{\cdot}3H_2O$ nanosheets the value is 44 ± 4%, consistent with the chemical stoichiometry. Therefore, for each treatment concentration approximately half the amount of copper is added for $Cu_3(PO_4)_2{\cdot}3H_2O$ then CuO.

Nanomaterial Characterization. Samples for nitrogen physisorption characterization with Brauner Emmet Teller (BET) analysis were degassed overnight at 120 °C under vacuum. The samples were analyzed using a Micrometrics Gemini VII 2390 surface analyzer (Norcross, GA) to measure nitrogen adsorption isotherms. Samples for X-ray powder diffraction were prepared by pressing the nanomaterials into a thin layer of Dow Corning vacuum grease (Midland, MI) on a zero-diffraction plate (B-doped Si, MTI Corporation). X-ray diffraction methods were collected using a Bruker Advance powder diffractometer (Spring TX) fitted with a Cu Kα source and a Lynxeye detector. The diffraction patterns were modified by subtracting the background and stripping the Kα_2 peaks using Bruker software DIFFRAC.EVA (Spring TX). Samples were prepared for scanning electron microscopy (SEM) by drop-casting a dilute solution of nanoparticles suspended in isopropyl alcohol on a conductive boron-doped silicon wafer. A LEO Supra55 VP field-emission scanning electron microscope (Zeiss, Germany) was used to obtain micrographs of the nanomaterials. Cu concentrations of nanomaterials were determined by digesting approximately 3 mg of the powders in 2 mL of *aqua regia* overnight. After the samples were diluted to a final volume of 10 mL, they were analyzed using inductively coupled optical emission spectroscopy (ICP-OES, PerkinElmer 4300 Dual View, Shelton CT).

Dissolution Experiments. We evaluated Cu metal release in suspensions of three different compositions: (1) deionized water (2) deionized water with a surfactant, and (3) a simulated xylem sap solution. Suspensions in (1) deionized water were prepared using of 100 mg/L CuO NP or $Cu_3(PO_4)_2{\cdot}3H_2O$ nanosheets prepared in deionized (DI) water (18 MΩ·cm, Barnstead nanopure systems) and adjusted to pH = 7 by adding HCl and NaOH until the desired pH was reached. Suspensions in (2) deionized water were performed in the same manner as those in deionized water, with the addition of 1

DOI: 10.1021/acssuschemeng.8b03379
ACS Sustainable Chem. Eng. 2018, 6, 14847−14856

mL/L of Regulaid nonionic surfactant (Kalo Inc., Overland Park, TX) adjusted to pH 7 through the addition of HCl and NaOH. Suspensions in (3) simulated xylem sap were performed by using a solution containing 890 μM malic acid and 1.71 mM citric acid, adjusted with NaOH to pH = 6. In some cases, 1 mL/L of Regulaid was added.[38] The simulated xylem sap contained chelating small organic acids and a lower pH to determine the impact of the plant environment on nanomaterial dissolution. To conduct ion release studies, triplicate samples of each CuO and $Cu_3(PO_4)_2{\cdot}3H_2O$ nanomaterials suspended in matrix (1), (2), (3) and (4) were placed under constant agitation at 100 rpm using New Brunswick C24 incubator shaker (Marshall Scientific, Cambridge MA) held at 30 °C and aliquots were sampled at specific intervals (1 h, 12 h, 24 h, 7 d, 21 d). Nanoparticles were removed from suspension by centrifugation at 5000 rpm, and the supernatant was then analyzed for Cu by inductively coupled plasma optical emission spectroscopy (ICP-OES, PerkinElmer 4300 Dual View, Shelton CT). Comparable studies were separately conducted at particle concentrations of 1000 mg/L in the pH 6 organic acid solution and in pH 7 DI water.

***In Vitro* Toxicity.** The toxicity of the two Cu nanomaterials to the pathogen *F. oxysporum* f. sp. *nivuem* was examined in shake culture. 50 mL of sterile potato dextrose broth (Difco Laboratories, Livonia, MI) was added to 125 mL Erlenmeyer flasks containing CuO NP or $Cu_3(PO_4)_2{\cdot}3H_2O$ nanosheets at concentrations of 50 and 500 mg/L, along with nanoparticle-free control samples. These Flasks were seeded with a colonized agar plug of *F. oxysporum* f. sp. *niveum* and were set on a platform shaker at 125 rpm for 5 d at 22 °C (INNOVA 2000, New Brunswick Scientific CO., INC. Edison, New Jersey, USA). Mycelial mats were harvested under vacuum onto preweighed Whatman #1 filter paper that had been dried at 50 °C for 18 h. The mycelia-containing filter papers were redried at 50 °C for at least 18 h and weighed. There were two replicate flasks per nanoparticle type and concentration. In addition, to determine the contribution of NP to the mass, additional controls were run without the fungus. These final weights were averaged by treatment and subtracted from the fungal weights to isolate the actual effect of NP on the pathogen.

Greenhouse Experiments. *Nanoparticle Exposure.* We selected watermelon infested with *F. oxysporum* as our model system to determine the disease suppression efficacy of CuO and $Cu_3(PO_4)_2$ nanomaterials. To perform these greenhouse studies, watermelon seeds (*Citrullus lanatus* Thunb. cv Sugar Baby, Harris Seed Co., Rochester, NY) were germinated in soilless potting mix (ProMix BX, Premier Hort Tech, Quakertown, PA) and fertilized once after 3 weeks with 40 mL of Peter's soluble 20−10−20 (N−P−K) fertilizer (R. J. Peters Inc., Allentown, PA). When plants reached the 3- to 4-leaf stage, uniform medium size plants were selected for NP exposure. Different concentrations of $Cu_3(PO_4)_2{\cdot}3H_2O$ nanosheets or CuO NP (both in suspension) were prepared in DI water (10−1000 mg/L). For CuO NP, the suspension was sonicated using a probe sonicator for 2 min in an ice bath. For $Cu_3(PO_4)_2{\cdot}3H_2O$ nanosheets, the suspension was sonicated in a bath sonicator for 5 min; this less intense sonication method was used out of concern over possible breakage of the nanosheets. Perhaps surprisingly, bath sonication of $Cu_3(PO_4)_2{\cdot}3H_2O$ nanosheets resulted in a more stable suspension than that achieved by more intense probe sonication CuO nanoparticles. Prior to exposure, one-to-two drops (1 mL/L) of Regulaid nonionic surfactant were added into the suspensions and a polyvinylidene chloride film (Saran wrap) was fitted around the stem to prevent the NP suspensions from entering the soil. In the greenhouse experiments, bulk CuO and $CuSO_4$ (Sigma, St. Louis, MO) were used to determine the effects of the nanomaterials independent of composition and Cu ion release. Four different treatment methods were used to determine the importance application method in delivering nanomaterials to the watermelon plant. The treatments were as follows: (1) dipping the foliage in to nanomaterial suspensions, (2) spraying foliage with the nanomaterial suspension (3) injecting the nanomaterial solution directly in to the root ball, and (4) repeated foliar applications of nanomaterials. Foliar application prevents against interactions between the nanomaterial and the soil that contains complexing organic acids, bacterial and fungal cultures. To study the influence of foliar application a "dip application" was used, where plants were inverted as shown in Figure S1. Each plant received approximately 0.6−0.8 mL of suspension as calculated by the volume difference from before and after exposure. The plants were then inverted and air-dried for 1 h prior to transplant. We note that the solutions were redispersed after treatment of 5 plants. Second, for foliar application, seedlings were sprayed with approximately 2 mL/plant of NP suspension. Third, at transplant to the infected growth media, select plants received a 5 mL amendment of one of the two NP solutions at either 500 or 1000 mg/L into the root ball/zone. Fourth, select plants received two separate foliar applications of the NP solutions at 20 or 200 mg/L; once at the initial transplant as above and a second after approximately 7 d of growth. The intent of these multiple applications was to compare repeated doses to roughly equivalent single treatments (i.e., two 20 mg/L doses vs a single 50 mg/L dose or two 200 mg/L doses against a single 500 mg/L dose).

Evaluation of Fusarium oxysporum Resistance. *F. oxysporum* f. sp. *niveum* was prepared on Japanese millet as previously described. The isolate of *Fusarium oxysporum* f. sp. *niveum* was cultured from infested watermelon seeds in Connecticut in 2014, and a colony originating from a single spore was stored at 4 °C. This isolate is considered highly virulent and has been used been used previously in our research.[39] NP-exposed and control seedlings were transplanted into potting mix infested with millet inoculum (0.75 g/L potting mix). There were 12 replicates in each NP treatment; 9 were infested with *F. oxysporum* and the remaining three were in pathogen-free soilless mix as noninoculated controls. All plants received 50 mL of a complete fertilizer solution (Peter's soluble 20−20−20 N, P, K) once per month and one application of imidacloprid (according to label instructions) (Bayer, Rhein, Germany) for insect control. As symptoms of fungal disease developed, plants were rated for severity on a scale of 1 to 5 where 1 = no disease, 2 = slightly stunted, 3 = stunted and or partially wilted, 4 = completely wilted and 5 = dead. The progress of disease as represented by the cumulative ratings of disease on replicate plants was plotted over time and the area-under-the-disease-progress curve (AUDPC) was calculated using the trapezoid rule:

$$\mathrm{AUDPC} = \sum [Y_i + Y_{(i+1)}]/2 \times (t_{(i+1)} - t_i) \quad (1)$$

where Y_i = the disease rating at time t_i.[40] After 6 to 8 weeks, depending on disease progress, the experiment was terminated. At harvest, the fresh shoot and root mass was separately recorded. All tissues were dried in an oven and acid digested for nutrient analysis (described below).

Field Experiments. Field experiments were conducted to evaluate if successful greenhouse results would translate to a field application. The following six treatments were established at two field locations (Hamden, CT - Location 1 and Griswold, CT - Location 2) to evaluate their effect on growth and *Fusarium* wilt of watermelon: (1) CuO nanoparticles, (2) $Cu_3(PO_4)_2{\cdot}3H_2O$ nanosheets, (3) commercially available CuO powder, (4) commercially available $Cu_3(PO_4)_2$ powder, (5) $CuSO_4$ and (6) untreated controls. Again, the primary purpose of this work was to compare the efficacy of the two nanoscale materials, and the bulk/salt materials were included to show the benefit of nanomaterials when compared to other Cu delivery approaches. Watermelon seeds ("Sugar Baby" Harris Seed Co. Rochester, NY) were germinated in 36 cell liners (1 plant/cell) filled with ProMix BX potting mix and were fertilized 3 weeks later with 40 mL of Peter's soluble 20−10−20 (N−P−K) fertilizer. Four-week-old transplants received a foliar application in the greenhouse with 1−2 mL of one of the six Cu treatments at 400 mg/L in distilled water that was amended with Regulaid (1 mL/L). All treatment solutions had been sonicated for at least 5 min in a FS20H Ultrasonic cleaner (Fisher Scientific Inc., Pittsburgh, PA) prior to application, except for CuO nanoparticles which were probe sonicated (Fisher Scientific, FB505) at 50% amplitude for 2 min.

Field microplots were prepared in early June 2017. Fertilizer (10−10−10, NPK) was spread over a 0.9 m wide rows at 112 kg/ha. The

DOI: 10.1021/acssuschemeng.8b03379
ACS Sustainable Chem. Eng. 2018, 6, 14847−14856

rows were set 6 m apart, covered in black plastic mulch and lined with irrigation drip tape. Rows were partitioned into 30 microplots (5.6 m^2). On June 30th (Location 2) and July fifth (Location 1), two transplants were set 30 cm apart in the center of each microplot. There were six replicate microplots/treatment. Planting holes were each infested with approximately 2 g of millet inoculum and hand mixed into the soil immediately before transplanting. In addition, another 30 microplots were planted immediately adjacent to these microplots and prepared the same way, but were not infested with the millet fungal inoculum. Plants were rated for disease three times on July 18th, August 11th, and Sept 7th for Location 2 and on July 19th, Aug 2nd and Aug 30th for Location 1, using the same scale (from 1 to 5) described above. Total plant biomass and fruit mass was determined at harvest; select tissues were dried for analysis by ICP mass spectrometry (ICP-MS) as noted below.

Tissue Elemental Analysis. Root and shoot tissue from greenhouse and field experiments (4−6 replicates per treatment, depending on experiment), as well as fruit tissue from field studies, were dried in an oven at 50 °C, ground in a Wiley mill, and passed through a 1 mm sieve. One medium watermelon fruit from each field plot was assayed to determine if the edible flesh portions had greater accumulation of Cu and other elements. Digestion of ground samples (0.5 g) was done in 50 mL polypropylene digestion tubes with 5 mL of concentrated nitric acid at 115 °C for 45 min using a hot block (DigiPREP System; SCP Science, Champlain, NY). The Ca, Cu, Fe, K, Mg, Mn, P, S, Si and Zn content was quantified using inductively coupled plasma optical emission spectroscopy (ICP-OES) on a Thermo Fisher iCAP 6500 (Thermo Fisher Scientific, Waltham, MA) or ICP with mass spectrometry (ICP-MS) on an Agilent 7500ce (Agilent, Santa Clara, CA); element content is expressed as μg/g (dry weight) plant tissue.

Pigment Analysis. Chlorophyll content was determined by the method of Lichtenthaler, with modification.[41] Briefly, 50 mg of fresh tissue was harvested, cut into pieces (<1 cm) and added to 15 mL centrifuge tubes amended with 10 mL of 95% ethanol. The tubes were kept in the dark for 3−5 d, and the chlorophyll content was measured by a UV−vis spectrophotometer (Spectronic Genesis 2). Concentrations of chlorophyll a (Chla), chlorophyll b (Chlb) and total chlorophyll were determined by the following equations: Chla = $13.36A_{664.2} - 5.19A_{648.6}$, Chlb = $27.43A_{648.6} - 8.12A_{664.2}$ and Total chlorophyll = Chla + Chlb.[41] Five replicates per treatment were analyzed.

Statistical Analysis. All data are presented as mean ± SE (standard error). A one-way analysis of variance (ANOVA) with the Student−Newman−Keuls (SNK) multiple comparison test was performed using SPSS (IBM SPSS Statistics version 20) to evaluate statistical significance. Differences were considered statistically significant when $p < 0.05$. A Student's t test was used for select analyses to determine statistical significance within a 95% confidence interval.

RESULTS AND DISCUSSION

Materials Characterization of CuO and $Cu_3(PO_4)_2$·$3H_2O$ Nanomaterials. The synthesized $Cu_3(PO_4)_2$·$3H_2O$ material had sheet-like morphology consistent with the anisotropic growth observed in $Cu_3(PO_4)_2$ protein inorganic complexes (Figure 1B).[31,32] The sheet-like morphology resulted in a relatively high specific surface area of 40 ± 1 m^2/g. A total of 165 exposed nanosheets were measured; the dimensions ranged from 53 to 608 nm, with a median value of 151 nm. The average nanosheet thickness as determined by atomic force microscopy (AFM) was 13 nm (±4; four replicate measurements). Figure 1C shows the powder diffraction pattern, which is well matched to JPSD00-022-0548, indicating the composition is $Cu_3(PO_4)_2$·$3H_2O$ nanosheets.[42] The synthesis of $Cu_3(PO_4)_2$·$3H_2O$ nanosheets allows for compositional comparison of the phosphate coordinating anion to the oxide. The commercial CuO nanoparticles aggregated in solution and showed an irregular morphology (Figure 1A), with a surface area of 12 ± 2 m^2/g; the X-ray power diffraction pattern is consistent with literature for a tenorite crystal structure (Figure 1D).[43]

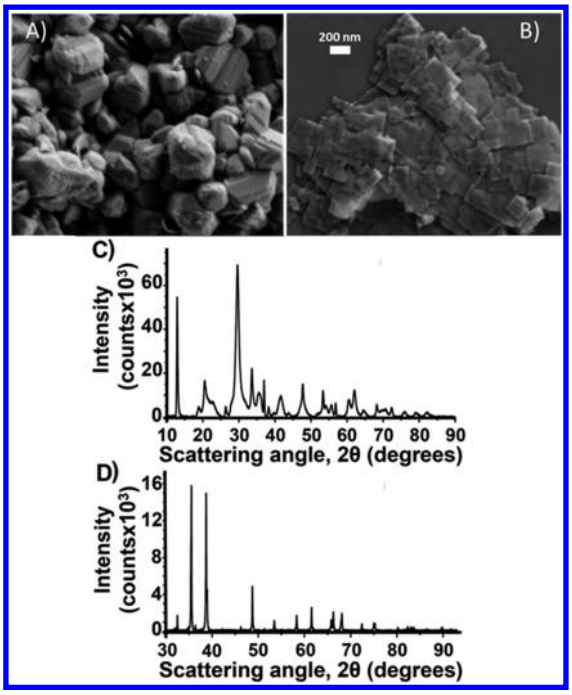

Figure 1. Micrographs and PXRD patterns of $Cu_3(PO_4)_2$·$3H_2O$ nanosheets (B, C) and commercial CuO nanoparticles (A, D). The scale bar is for both panels A and B.

Dissolution Experiments. Dissolution experiments for the two nanomaterials were conducted: (1) deionized water, (2) deionized water and Regulaid, (3) simulated xylem sap and (4) simulated sylem sap and Regulaid (Figure 2). Figure 2A shows the concentration of Cu^{2+} ions produced from dissolution of the different nanoparticles. Figure 2A shows that the $Cu_3(PO_4)_2$·$3H_2O$ nanosheets had a rapid initial release of ions across the media studied, reaching a constant value after 12 h. The slight decrease over time in Figure 2A,B may be due to minimal Cu ion reprecipitation as both copper phosphate or copper hydroxide species. Conversely, the commercial CuO nanoparticles showed continual ion release from the particles over the five-week study period. After 1 week, $Cu_3(PO_4)_2$·$3H_2O$ nanosheets had released more Cu ions in to solution than CuO nanoparticles, with values of 15 ± 2.0 μM and 7.0 ± 0.6 μM, respectively (Figure 2A). For CuO nanoparticles, a similar slow release profile of extractable Cu ions from nanomaterials incubated in soil has been previously reported.[44] The presence of Regulaid in the solution reduced ion release from both CuO nanoparticles and $Cu_3(PO_4)_2$·$3H_2O$ nanosheets, with similar maximum copper concentrations in solution of 9 ± 2 μM and 8.7 ± 0.5 μM, respectively (Figure 2B). The addition of the organic acids at concentrations approximating plant xylem levels dramatically increased the dissolved copper content by 2 orders of magnitude, reaching 1110 ± 30 μM and 1010 ± 40 μM for CuO nanoparticles and $Cu_3(PO_4)_2$·$3H_2O$ nanosheets after 1 week, respectively. Furthermore, there was significantly more Cu leached from CuO under these conditions (Figure 2B). We hypothesize that the Regulaid prevents particle dissolution by stabilizing the nanomaterial dispersion within the solution. Alternatively, the

DOI: 10.1021/acssuschemeng.8b03379
ACS Sustainable Chem. Eng. 2018, 6, 14847−14856

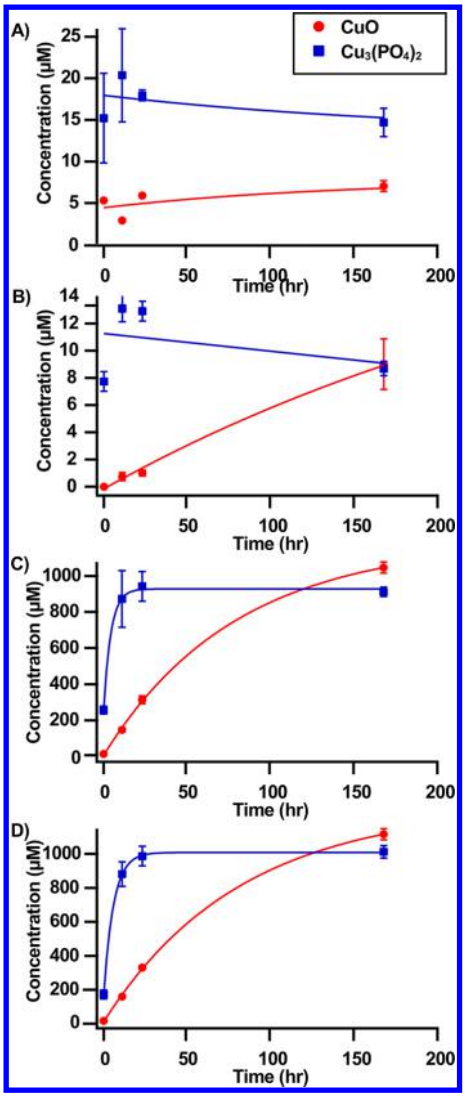

Figure 2. Concentration of Cu^{2+} in solution vs time after the indicated nanomaterials was introduced into different media at a mass concentration of 100 mg/L of. Media shown are (A) deionized water, (B) Regulaid, (C) malic and citric acid mixture and (D) malic and citric acid mixture with added Regulaid. Lines were generated from an exponential fit to the data.

organic acids in the simulated xylem sap mat chelate the copper ions in solution and drive the dissolution process in the forward direction, given the reported favorable binding constants of 1.299×10^4 and 1.801×10^4 M^{-1} between copper nanomaterials and malic and citric acid, respectively.[11] Notably, the presence of Regulaid did not significantly reduce ion release in the presence of simulated xylem sap (Figure 1D). Previously, the dissolution behavior of CuO films has been characterized in acidic citric acid solutions which showed Cu concentrations of <10 mg/L near pH = 7, increasing at lower pH.[45] The addition of soluble proteins and yeast extract has also been shown to enhance Cu ion release for CuO.[46] To determine whether the solution was saturating, comparable dissolution studies were performed at 1000 mg/L in deionized water and the organic acid matrix (Figure S2). When compared to the 100 mg/L experiment, the 1000 mg/L study showed an increase in the ion release from $Cu_3(PO_4)_2 \cdot 3H_2O$ nanosheets by at least a factor of 2 in both matrices, while CuO showed relatively small changes in the profile observed, indicating that equilibrium may be established at lower concentrations (Figure S2). To our knowledge, the dissolution characteristics of $Cu_3(PO_4)_2 \cdot 3H_2O$ nanosheets have not been previously reported. The results of these studies show that $Cu_3(PO_4)_2$ and CuO nanomaterials have different ion release profiles, with $Cu_3(PO_4)_2$ initially releasing more ions than CuO. The ion release profile of the materials may be related to the disease suppression efficacy reported in later sections. In addition, the results of dissolution studies show that ion release from both CuO and $Cu_3(PO_4)_2$ nanomaterials may be stimulated after the nanomaterials enter the plant tissues and contact xylem sap.

***In Vitro* Toxicity.** To determine whether the nanomaterials could directly influence the health of *F. oxysporum*, a direct assay of fungal toxicity was performed. In the fungal toxicity test, pathogen biomass was not significantly impacted by the presence of CuO nanoparticles at concentrations of 50 and 500 mg/L in the growth medium. Conversely, fungal biomass was significantly reduced by $Cu_3(PO4)_2 \cdot 3H_2O$ nanosheets at concentrations of 50 and 500 mg/L by 20 and 40%, respectively. These findings in conjunction with the dissolution data may suggest that the more rapid release of ions from the $Cu_3(PO_4)_2$ nanosheets results in greater direct disease suppression. However, using foliar application of the nanomaterials on plants requires that the particles must translocate through the plant to have a direct interaction with the fungal culture. Therefore, *in vitro* studies may not reflect the observations noted in the greenhouse or field.

Greenhouse Studies. Dip and Root Application of Nanomaterials. To compare the disease suppression of Cu-based nanomaterial treatments at 10−1000 mg/L applied concentrations to an infected control that was not treated with nanomaterials, a "dip" method was used on the seedlings. This exposure method enabled a more controlled and homogeneous application of the nanomaterials to the entire shoot system. To assess the progress of *Fusarium* infection during plant growth, the area under the disease progress curve (AUDPC) was calculated, with higher values representing greater disease progression and vegetative damage. In Figure 3A, the commercial CuO NP showed a downward trend in disease progression with increasing concentration but statistically significant *Fusarium* suppression (50.6%) was only achieved at a dose of 1000 mg/L. Conversely, a 10 mg/L treatment of $Cu_3(PO_4)_2 \cdot 3H_2O$ nanosheets exhibited a statistically significant 58% reduction in AUDPC, with higher doses providing no additional effect (Figure 3A). Based on the stoichiometry and as determined experimentally, CuO is 85 ± 6% Cu by mass, while $Cu_3(PO_4)_2 \cdot 3H_2O$ is 44 ± 4%, respectively. Therefore, each applied dose of $Cu_3(PO_4)_2$ contains roughly half the amount of Cu when compared to CuO and shows disease suppression efficacy at 100 times lower concentrations. Importantly, the repeated application of CuO nanoparticles produced a significant reduction in the AUDPC; dual doses of 20 and 200 mg/L resulted in 46.5% and 40.3% reductions in disease (Figure 3C). For the $Cu_3(PO_4)_2 \cdot 3H_2O$ nanosheets, the repeated application regime yielded similar resistance to disease as did the single dose at 10 mg/L.

The wet mass of the plant was also used to assess plant health. The root, shoot and total plant wet mass were determined as a function of Cu treatment. *Fusarium* infection reduced watermelon biomass by 80.9%. For the commercial CuO nanoparticles, increasing dose showed an increase in plant biomass; however, unlike AUDPC, these values were not

DOI: 10.1021/acssuschemeng.8b03379
ACS Sustainable Chem. Eng. 2018, 6, 14847−14856

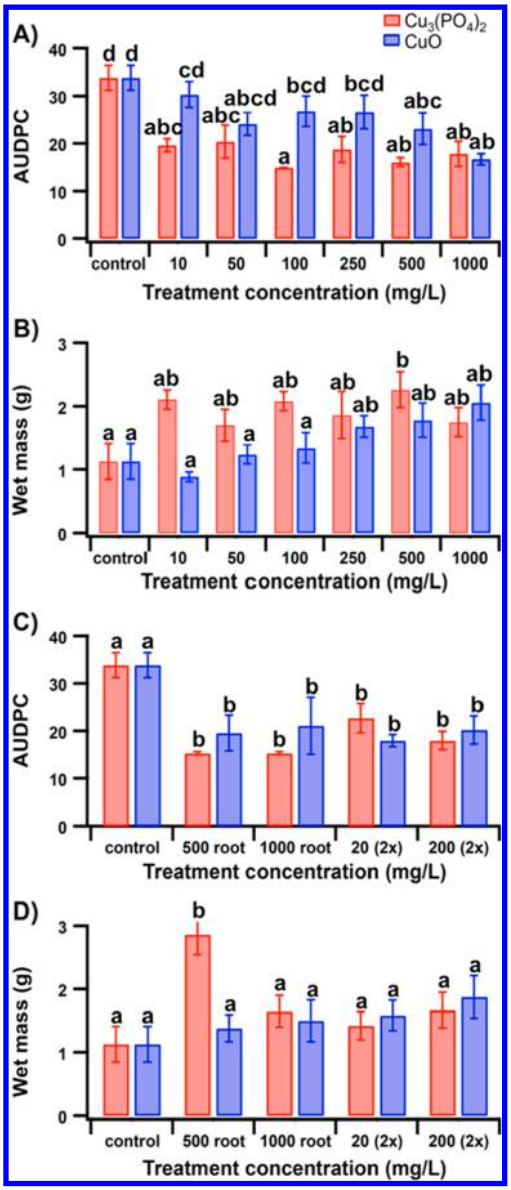

Figure 3. Disease rating and fresh weight of *Fusarium* infested watermelon upon exposure to $Cu_3(PO_4)_2{\cdot}3H_2O$ nanosheets and CuO NP: (A) reduction of the area under the disease progress curve (AUDPC) with respect to foliar nanoparticle treatments; (B) changes in total wet mass with respect to foliar treatment; (C) change in the AUDPC with respect to repeated foliar treatment and root applications of CuO NP and $Cu_3(PO_4)_2{\cdot}3H_2O$ nanosheets; (D) changes in total wet mass with respect to repeated foliar applications and root exposure. For the repeated applications, "2x" indicates two separate foliar treatments of either 20 or 200 mg/L. A one-way ANOVA with a SNK multiple comparison test was used to determine significance across all the treatments. Values in each panel followed by different letters are significantly different at $p < 0.05$.

statistically significant, even at a dose of 1000 mg/L (Figure 3B). Conversely, treatment with $Cu_3(PO_4)_2{\cdot}3H_2O$ nanosheets at 10 mg/L resulted in a statistically significant increase in the biomass of plants infected with *Fusarium*. These findings were consistent with the AUDPC data. Although the higher doses of $Cu_3(PO_4)_2{\cdot}3H_2O$ nanosheets consistently produced greater biomass values, a high degree of replicate variability occasionally confounded statistical significance. In terms of biomass, the repeated applications at 20 or 200 mg/L of either particle type offered no additional resistance to infection.

The nanomaterials were also applied directly into the root zone. Here, we observed a similar lack of effect of CuO nanoparticles at both doses and of the nanosheets at 1000 mg/L for the root application, with respect to biomass (Figure 3D). However, the 500 mg/L root treatment with $Cu_3(PO_4)_2{\cdot}3H_2O$ nanosheets resulted in a dramatic 261% increase in total plant biomass. These results demonstrate that the $Cu_3(PO_4)_2{\cdot}3H_2O$ nanosheets effectively reduce disease at low particle concentrations, without the need for repeated applications, whereas the commercial CuO NP were only partially effective at much higher doses.

Nutrient Analysis. The content of both macro- (Ca, P, S, K and Mg) and micronutrients (Cu, Fe, Zn, Mn and Si) were measured in watermelon shoots and roots across all treatments (Figure 4, Table S1 and S2). As shown in Figure 4A, the shoot

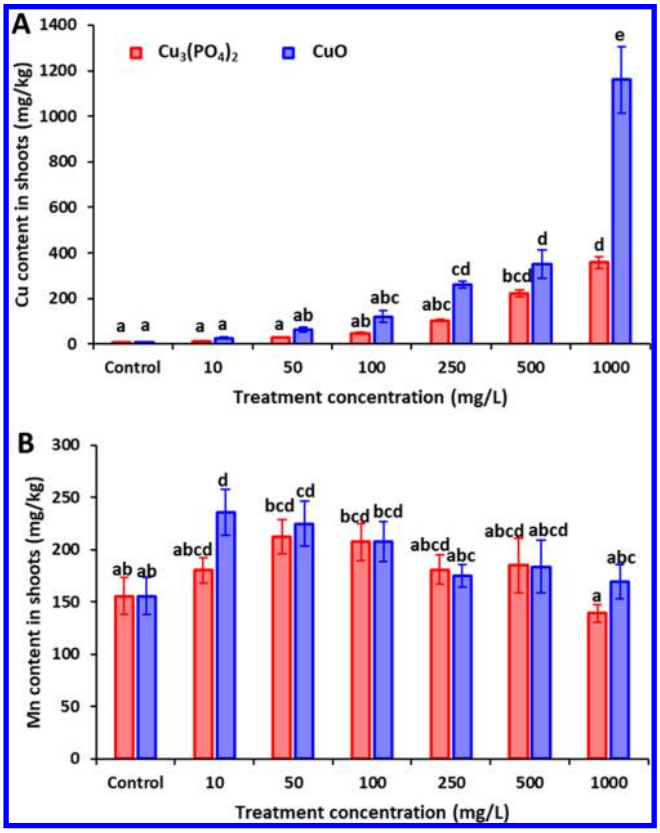

Figure 4. Cu (A) and Mn (B) content in *Fusarium* infected watermelon shoots upon foliar exposure to different concentrations of $Cu_3(PO_4)_2{\cdot}3H_2O$ nanosheets and CuO nanoparticles. A one-way ANOVA with an SNK multiple comparison test was used to determine significance across all the treatments. Values in each panel followed by different letters are significantly different at $p < 0.05$.

Cu content in diseased plants increased in a dose-dependent fashion with increasing treatment of Cu-based nanomaterials. The consistently higher levels of shoot Cu for the commercial CuO NP are the result of the greater mass fraction of this element in the molecule relative to the $Cu_3(PO_4)_2{\cdot}3H_2O$ nanosheets. If the data were normalized to amount of Cu applied, minimal differences between the two materials would be observed. For all plants exposed to *F. oxysporum*, the addition of Cu based nanomaterials lead to a decrease in the

DOI: 10.1021/acssuschemeng.8b03379
ACS Sustainable Chem. Eng. 2018, 6, 14847−14856

root content of Cu when compared to the *F. oxysporum* infested control (Table S2), although not all changes were of statistical significance. Our findings do not align with previous studies on CuO nanomaterials with a primary particle size of 30 nm.[13,39] While the reasons for these differences remain unknown, it is possible that the larger aggregate size of our current CuO nanoparticles may limit translocation from the shoot to the root. In the healthy plants, the shoot Cu content increased in a dose-dependent manner, which was similar to the *Fusarium* infested treatments (Table S2). Regarding other mineral elements, it is interesting to note that the root P content in the *Fusarium* infested treatments with both types of Cu nanomaterials was decreased as compared to the control (Table S1). For example, exposure to 50, 100 and 500 mg/L CuO nanoparticles greatly decreased the root P content by 14.2−21.4% relative to the *Fusarium* control. Similarly, the presence of CuO nanoparticles significantly decreased the *Fusarium* infested root K and S content (Table S1). For micronutrient content, exposure to both $Cu_3(PO_4)_2{\cdot}3H_2O$ nanosheets and CuO nanoparticles at lower levels significantly elevated the shoot Mn content in the *Fusarium* infested treatments as compared to the *Fusarium* control (Figure 4B). In addition, the presence of CuO nanoparticles increased the shoot Si content upon infection (Table S2). Si is known to play an important role in plant defense by interacting with the plant stress signaling system and controlling the timing of disease responses.[47] The lack of Si change under $Cu_3(PO_4)_2{\cdot}3H_2O$ treatment suggests an overall alleviation of stress in the diseased condition relative to the CuO NP exposure.

Foliar Spray of Nanomaterials. *Growth and Disease Suppression.* In green house trials, a foliar spray method of CuO NP and $Cu_3(PO_4)_2{\cdot}3H_2O$ nanosheets was undertaken to investigate the impact of different application methods on disease response and yield. In the absence of disease, the nanomaterial amendments had no impact on total plant biomass; the total plant wet mass across all treatments ranged from 10.8 to 12.2 g (Figure S3). The CuO nanoparticles slightly reduced the vine length of the watermelon plants by approximately 15%. Under disease conditions, total biomass and vine length of the nanomaterial-free control was reduced by more than 55%. Although treatment with CuO NP and $CuSO_4$ had no impact, $Cu_3(PO_4)_2{\cdot}3H_2O$ nanosheets significantly alleviated the decrease in vine length, resulting in values that were statistically similar to the controls (Figure S4). Under disease conditions, the CuO and $Cu_3(PO_4)_2{\cdot}3H_2O$ nanomaterials significantly reduced the AUDPC by 23 and 25%, respectively, as compared to the controls, bulk and ionic copper treatments (Figure S5). Both $Cu_3(PO_4)_2{\cdot}3H_2O$ nanosheets and CuO NP increased plant mass by approximately 40% relative to the diseased controls, although the change was only statistically significant for the CuO (Figure S3). There was greater consistent variability in both biomass and AUDPC in this experiment with the foliar spray. It is likely that the foliar application method resulted in less uniform and incomplete coverage of Cu materials on the plant shoot system as compared to the dip method, thereby resulting in greater variability in treatment efficacy. In addition, another reason for the variability between the AUDPC and biomass is that the AUDPC was generated from ratings taken during growth when significant delays in the onset of symptoms were evident in the $Cu_3(PO_4)_2{\cdot}3H_2O$ nanosheets treatment, whereas total biomass was recorded at final harvest when the disease had progressed in all inoculated treatments, thus reducing the likelihood of any differences being detected.

Pigment Analysis. In this experiment, the impact of disease and treatment on pigment production was also assessed; changes in pigment concentrations can be an indicator of plant stress.[48] In the absence of nanomaterials, the total chlorophyll and carotenoid content significantly increased from 0.7 ± 0.02 mg/g to 0.9 ± 0.2 mg/g in response to disease (Figure S6). For uninfected plants, the addition of $Cu_3(PO_4)_2{\cdot}3H_2O$ nanosheets, CuO nanoparticles and $CuSO_4$ significantly increased total chlorophyll and carotenoid content. Under disease conditions, $CuSO_4$ and CuO NP did not significantly change the chlorophyll content when compared to the 0.9 ± 0.2 mg/g of the diseased control, while significantly less chlorophyll was observed for $Cu_3(PO_4)_2{\cdot}3H_2O$ nanosheets with a value of 0.70 ± 0.08 mg/g. For the healthy plants, the increased pigment concentration may be an indication of decreased plant stress and robust plant health. Conversely, in the diseased plants, the decreased chlorophyll in response to $Cu_3(PO_4)_2{\cdot}3H_2O$ nanosheets may indicate that the rapid dissolution of ions interferes with chlorophyll biosynthesis.[26,48]

Field Studies. Full life cycle studies were performed at two separate field sites to determine whether the results of the greenhouse studies would translate to a practical field agricultural application. At both field locations, the CuO and $Cu_3(PO_4)_2{\cdot}3H_2O$ nanomaterials significantly reduced the AUDPC when compared to the diseased control, although the two chemical compositions yielded results that were statistically equivalent to each other. At location 1, Figure 5 shows that the CuO and $Cu_3(PO_4)_2{\cdot}3H_2O$ nanoparticles reduced disease by 29.9% and 39.2%, respectively. Similarly, measurements at location 2 showed that treatment with $Cu_3(PO_4)_2{\cdot}3H_2O$ reduced disease by 34%; no CuO NP treatment was established at location 2. The nanomaterial results were compared to Cu ions produced by a $CuSO_4$ salt control; these two treatments were shown to be statistically equivalent.

Fruit Productivity. At both locations, the presence of disease reduced crop yield (total wet mass of fruit per replicate plot) by 34.8% (from 10.9 ± 1.1 kg to 7.1 ± 1.1 kg) and 57.1% (from 12.6 ± 1.8 kg to 5.4 ± 1.6 kg), respectively. At location 1, in the presence of disease the CuO nanoparticle treatment increased yield by 29% when compared to the diseased control, resulting in a value that was statistically equivalent to the untreated controls (Figure 5B). The $Cu_3(PO_4)_2{\cdot}3H_2O$ nanosheets and $CuSO_4$ salt control offered no such benefit on total yield. Disease reduced the average mass of per fruit from 2.30 to 1.90 kg; under disease conditions, treatment with $Cu_3(PO_4)_2{\cdot}3H_2O$ restored the average per fruit mass to 2.70 kg. At location 2, the $Cu_3(PO_4)_2{\cdot}3H_2O$ and $CuSO_4$ salt control treatments increased fruit yield by 38.2%, although large replicate variability resulted in a lack of statistical significance (Figure 5C).

Elemental Analysis. Elemental analysis was conducted on the roots, shoots and fruit of plants from both field locations (Tables S3−S6). In general, changes with nanoscale treatment were minimal. For the fruit from the field study at both locations, there appeared to be no increase in fruit Cu content with respect to nanoparticle treatment, which may be due to the fact that nanomaterials were applied to the foliage several months before harvest. In addition, at location 1 the fruit treated with the CuO nanoparticles showed reduced content of Zn, Si, S, P, Mn, Mg, K and Fe. Conversely, the fruits of plants

DOI: 10.1021/acssuschemeng.8b03379
ACS Sustainable Chem. Eng. 2018, 6, 14847−14856

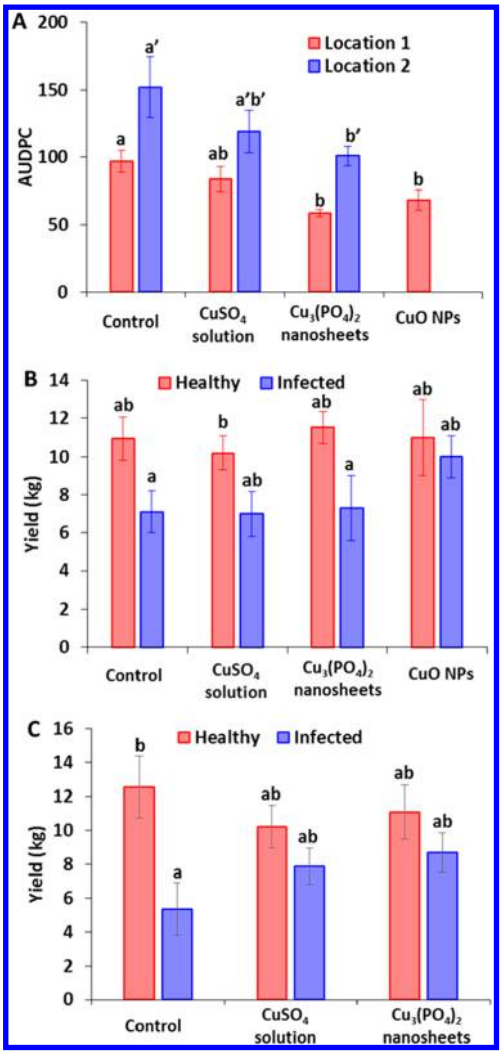

Figure 5. Disease progress and yield of *Fusarium* infested watermelon in Lockwood and Griswold field studies. Panel A represents disease progress for the Lockwood (Location 1) and Griswold (Location 2) using applications of CuO NP and $Cu_3(PO_4)_2{\cdot}3H_2O$ nanosheets compared to a $CuSO_4$ salt control. CuO NP were not used in Griswold field. Panels B and C represent the total yield of Cu-based nanomaterial treated watermelon w/or w/o *Fusarium* infection for the Lockwood and Griswold locations, respectively. A one-way ANOVA with a SNK multiple comparison test was used to determine significance across all the treatments. For panel A, the analysis was within a location. For panels B and C, the analysis was across are treatments. Values in each panel followed by different letters are significantly different at $p < 0.05$.

treated with $Cu_3(PO_4)_2{\cdot}3H_2O$ nanosheets showed increased concentrations of Si, Mn, Mg, Fe and Ca and had reduced concentrations of Zn, S, P, Cu and K. Furthermore, in response to disease, plants at location 1 showed decreased shoot Mg and Fe, increases in the root Cu and Ca concentration and decreases in root Si and Fe. Under disease conditions, the nanomaterials increased the Mn content and CuO NP increased the Fe content. At location 2, shoot Cu, Mg and S content decreased and shoot Mn increased with respect to disease. No noticeable changes were observed in the roots. In response to $Cu_3(PO_4)_2{\cdot}3H_2O$ nanosheets, there was an increase in the shoot Zn content.

Environmental Implications. Taken together, the greenhouse and field studies demonstrate the significant potential for nanoscale Cu treatments to suppress fungal root infection and sustainably promote overall plant health and perhaps yield. Cu has been widely used in traditional agricultural practices to repress disease. However, the high volumes of Cu currently used has led to concerns about environmental accumulation of this metal, as well as the development of resistance among pathogens. The development of nanoscale Cu delivery systems that could suppress disease and increase yield at lower active nutrient concentrations would be a significant achievement. Foliar application of commercial nanoscale CuO has been shown to suppress *Fusarium* and *Verticillium* wilt of tomato and eggplant, respectively, and increase the biomass and fruit yield in controlled laboratory settings.[13] Furthermore, foliar application of CuO nanoparticles in the presence of disease was correlated with an up-regulation of gene expression of polyphenol oxidase, which is involved in the nonspecific defense reactions that protect plants against pathogens.[39] Nanoscale properties are clearly important to the efficacy of Cu treatment, with the materials showing effectiveness with a variety of species, including the 53% reduction of red root rot disease in tea.[49] To further enhance the effectiveness of nanomaterial treatments, effort should be focused on optimization of the nanomaterial composition, structure and activity. For instance, Cu nanocomposites, including core−shell Si−Cu, multivalent Cu and quaternary ammonium stabilized Si−Cu composites, have shown increased disease suppression on tomato bacterial spot (*Xanthomonas perforans*) when compared to commercially available Kocide.[4] Similarly, the findings of the current study show the significance of nanomaterial formulation. The $Cu_3(PO_4)_2{\cdot}3H_2O$ nanosheets are significantly more effective than CuO NP, with 100× less mass needed to produce the same result in greenhouse studies, and nearly half the amount of Cu delivered on a per gram basis. The results of these studies should stimulate investigations to optimize efficacy as a function of elemental structure, as well as to understand nanoparticle−plant surface interactions and the particle dissolution profile.

CONCLUSIONS

In summary, $Cu_3(PO_4)_2{\cdot}3H_2O$ nanosheets and commercial CuO NP were applied to watermelon plants infected with *Fusarium* wilt to determine the role of ion release profile and nanomaterial composition/structure on disease suppression in greenhouse and field studies. The greenhouse studies indicate that the $Cu_3(PO_4)_2{\cdot}3H_2O$ nanosheets reduce disease at a significantly lower mass concentration of particles as compared to CuO NP. The efficacy of the materials may be attributed to the reduced overall particle size, unique particle structure (sheets) and more rapid initial release of ions from $Cu_3(PO_4)_2{\cdot}3H_2O$ nanosheets compared to the CuO NP. Both Cu nanomaterials exhibited similar efficacy in field trials involving full life cycle plant growth, in spite of the fact that the amendment occurred only once at the seedling stage. These results indicate that the $Cu_3(PO_4)_2{\cdot}3H_2O$ nanosheets and similar materials hold great promise for agricultural applications. However, the present variability in the particle morphology, surface area and size motivates mechanistic studies to understand how these materials interact with the plant-pathogen system.

DOI: 10.1021/acssuschemeng.8b03379
ACS Sustainable Chem. Eng. 2018, 6, 14847−14856

■ ASSOCIATED CONTENT

Supporting Information

The Supporting Information is available free of charge on the ACS Publications website at DOI: 10.1021/acssuschemeng.8b03379.

This information includes additional details on particle dissolution studies, as well as the elemental and pigment content of greenhouse and field watermelon tissues (PDF)

■ AUTHOR INFORMATION

Corresponding Authors

*J. C. White. E-mail: Jason.White@ct.gov (Tel, Fax: 203-974-8523).

*R. J. Hamers. E-mail: rjhamers@wisc.edu (Tel, Fax: 608-262-6371).

ORCID

Chuanxin Ma: 0000-0001-5125-7322

Natalie Hudson-Smith: 0000-0002-2642-0711

Christy L. Haynes: 0000-0002-5420-5867

Jason C. White: 0000-0001-5001-8143

Robert J. Hamers: 0000-0003-3821-9625

Notes

The authors declare no competing financial interest.

■ ACKNOWLEDGMENTS

This work was supported by the National Science Foundation Centers for Chemical Innovation Program CHE-1503408, the Center for Sustainable Nanotechnology. C.D.P.P. acknowledges the Federal University of Lavras Doctoral Exchange Scholarship Program. ICP-OES and ICP-MS work done by R.D.L.T.-R. and N.Z.-M. was supported by USDA-NIFA-AFRI 2016-67021-24985 and FDA 1U18FD005505-03, respectively.

■ REFERENCES

(1) United Nations. *World Population Prospects: The 2015 Revision, Key Findings and Advance Tables*; Department of Economics and Social Affairs, United Nations, 2015.

(2) Rodrigues, S. M.; Demokritou, P.; Dokoozlian, N.; Hendren, C. O.; Karn, B.; Mauter, M. S.; Sadik, O. A.; Safarpour, M.; Unrine, J. M.; Viers, J.; Welle, P.; White, J. C.; Wiesner, M. R.; Lowry, G. V. Nanotechnology for sustainable food production: promising opportunities and scientific challenges. *Environ. Sci.: Nano* **2017**, *4* (4), 767−781.

(3) Servin, A.; Elmer, W.; Mukherjee, A.; De la Torre-Roche, R.; Hamdi, H.; White, J. C.; Bindraban, P.; Dimkpa, C. A review of the use of engineered nanomaterials to suppress plant disease and enhance crop yield. *J. Nanopart. Res.* **2015**, *17* (2), 21.

(4) Strayer-Scherer, A.; Liao, Y. Y.; Young, M.; Ritchie, L.; Vallad, G. E.; Santra, S.; Freeman, J. H.; Clark, D.; Jones, J. B.; Paret, M. L. Advanced Copper Composites Against Copper-Tolerant Xanthomonas perforans and Tomato Bacterial Spot. *Phytopathology* **2018**, *108* (2), 196−205.

(5) Kumar, S. A.; Ilango, P. The impact of wireless sensor network in the field of precision agriculture: a review. *Wireless Personal Communications* **2018**, *98* (1), 685−698.

(6) Savary, S.; Ficke, A.; Aubertot, J.-N.; Hollier, C. *Crop losses due to diseases and their implications for global food production losses and food security*; Springer, 2012; DOI: 10.1007/s12571-012-0200-5.

(7) Dordas, C. Role of nutrients in controlling plant diseases in sustainable agriculture. A review. *Agron. Sustainable Dev.* **2008**, *28* (1), 33−46.

(8) Nunes, I.; Jacquiod, S.; Brejnrod, A.; Holm, P. E.; Johansen, A.; Brandt, K. K.; Prieme, A.; Sorensen, S. J. Coping with copper: legacy effect of copper on potential activity of soil bacteria following a century of exposure. *Fems Microbiology Ecology* **2016**, *92* (11), fiw175.

(9) Sims, J. T. Soil-pH effects on the distribution and plant availability of manganese, copper, and zinc. *Soil Science Society of America Journal* **1986**, *50* (2), 367−373.

(10) Servin, A. D.; White, J. C. Nanotechnology in agriculture: Next steps for understanding engineered nanoparticle exposure and risk. *Nanoimpact* **2016**, *1*, 9−12.

(11) Huang, Y. X.; Zhao, L. J.; Keller, A. A. Interactions, Transformations, and Bioavailability of Nano-Copper Exposed to Root Exudates. *Environ. Sci. Technol.* **2017**, *51* (17), 9774−9783.

(12) Ingle, A. P.; Rai, M. Copper nanoflowers as effective antifungal agents for plant pathogenic fungi. *IET Nanobiotechnol.* **2017**, *11* (5), 546−551.

(13) Elmer, W. H.; White, J. C. The use of metallic oxide nanoparticles to enhance growth of tomatoes and eggplants in disease infested soil or soilless medium. *Environ. Sci.: Nano* **2016**, *3* (5), 1072−1079.

(14) Liu, R. Q.; Lal, R. Potentials of engineered nanoparticles as fertilizers for increasing agronomic productions. *Sci. Total Environ.* **2015**, *514*, 131−139.

(15) Dimkpa, C. O.; Bindraban, P. S. Fortification of micronutrients for efficient agronomic production: a review. *Agron. Sustainable Dev.* **2016**, *36* (1), 7.

(16) Lefiles, J. H.; Taylor, E. J.; Crawford, M. A. Copper hydroxide dry flowable bactericide/fungicide and method of making and using same. U.S. Patent 5,462,738, 1994.

(17) Hoang, T. C.; Rogevich, E. C.; Rand, G. M.; Gardinali, P. R.; Frakes, R. A.; Bargar, T. A. Copper desorption in flooded agricultural soils and toxicity to the Florida apple snail (Pomacea paludosa): Implications in Everglades restoration. *Environ. Pollut.* **2008**, *154* (2), 338−347.

(18) Baldi, E.; Miotto, A.; Ceretta, C. A.; Quartieri, M.; Sorrenti, G.; Brunetto, G.; Toselli, M. Soil-applied phosphorous is an effective tool to mitigate the toxicity of copper excess on grapevine grown in rhizobox. *Sci. Hortic.* **2018**, *227*, 102−111.

(19) Behlau, F.; Belasque, J.; Graham, J. H.; Leite, R. P. Effect of frequency of copper applications on control of citrus canker and the yield of young bearing sweet orange trees. *Crop Prot.* **2010**, *29* (3), 300−305.

(20) Cioffi, N.; Torsi, L.; Ditaranto, N.; Tantillo, G.; Ghibelli, L.; Sabbatini, L.; Bleve-Zacheo, T.; D'Alessio, M.; Zambonin, P. G.; Traversa, E. Copper nanoparticle/polymer composites with antifungal and bacteriostatic properties. *Chem. Mater.* **2005**, *17* (21), 5255−5262.

(21) Mantecca, P.; Moschini, E.; Bonfanti, P.; Fascio, U.; Perelshtein, I.; Lipovsky, A.; Chirico, G.; Bacchetta, R.; Del Giacco, L.; Colombo, A.; Gedanken, A. Toxicity Evaluation of a New Zn-Doped CuO Nanocomposite With Highly Effective Antibacterial Properties. *Toxicol. Sci.* **2015**, *146* (1), 16−30.

(22) Rajasekaran, P.; Kannan, H.; Das, S.; Young, M.; Santra, S. Comparative analysis of copper and zinc based agrichemical biocide products: materials characteristics, phytotoxicity and in vitro antimicrobial efficacy. *Aims Environmental Science* **2016**, *3* (3), 439−455.

(23) Zhao, L. J.; Hu, Q. R.; Huang, Y. X.; Keller, A. A. Response at Genetic, Metabolic, and Physiological Levels of Maize (Zea mays) Exposed to a Cu(OH)2 Nanopesticide. *ACS Sustainable Chem. Eng.* **2017**, *5* (9), 8294−8301.

(24) Elmer, W. H.; White, J. C. The use of metallic oxide nanoparticles to enhance growth of tomatoes and eggplants in disease infested soil or soilless medium. *Environ. Sci.: Nano* **2016**, *3* (5), 1072−1079.

(25) Iqbal, J.; Jan, T.; Ul-Hassan, S.; Ahmed, I.; Mansoor, Q.; Ali, M. U.; Abbas, F.; Ismail, M. Facile synthesis of Zn doped CuO hierarchical nanostructures: Structural, optical and antibacterial properties. *AIP Adv.* **2015**, *5* (12), 127112.

(26) Zhao, L. J.; Hu, J.; Huang, Y. X.; Wang, H. T.; Adeleye, A.; Ortiz, C.; Keller, A. A. H-1 NMR and GC-MS based metabolomics reveal nano-Cu altered cucumber (Cucumis sativus) fruit nutritional supply. *Plant Physiol. Biochem.* **2017**, *110*, 138−146.
(27) Weng, D.; Jokiel, P.; Uebleis, A.; Boehni, H. Corrosion and protection characteristics of zinc and manganese phosphate coatings. *Surf. Coat. Technol.* **1997**, *88* (1−3), 147−156.
(28) Cohen, Y.; Coffey, M. D. Systemic fungicides and the control of oomycetes. *Annu. Rev. Phytopathol.* **1986**, *24* (1), 311−338.
(29) Thizy, A.; Pillon, D.; Debourge, J.-C.; Lacroix, G. Fungicidal compositions containing phosphorous acid and derivatives thereof. U.S. Patent 4119724A, 1978.
(30) Duan, L. L.; Wang, H. X.; Hou, J. W.; Zhang, Y. T.; Chen, V. A facile, bio-inspired synthetic route toward flower-like copper phosphate crystals with high specific surface area. *Mater. Lett.* **2015**, *161*, 601−604.
(31) Escobar, S.; Velasco-Lozano, S.; Lu, C. H.; Lin, Y. F.; Mesa, M.; Bernal, C.; Lopez-Gallego, F. Understanding the functional properties of bio-inorganic nanoflowers as biocatalysts by deciphering the metal-binding sites of enzymes. *J. Mater. Chem. B* **2017**, *5* (23), 4478−4486.
(32) Li, Z. X.; Ding, Y.; Wu, X. L.; Ge, J.; Ouyang, P. K.; Liu, Z. An enzyme-copper nanoparticle hybrid catalyst prepared from disassembly of an enzyme-inorganic nanocrystal three-dimensional nanostructure. *RSC Adv.* **2016**, *6* (25), 20772−20776.
(33) Wang, J.; Zhu, T.; Ho, G. W. Nature-Inspired Design of Artificial Solar-to-Fuel Conversion Systems based on Copper Phosphate Microflowers. *ChemSusChem* **2016**, *9* (13), 1575−1578.
(34) Wu, X. F.; Shi, G. Q.; Wang, S. B.; Wu, P. Y. Formation of 3D dandelions and 2D nanowalls of copper phosphate dihydrate on a copper surface and their conversion into a nanoporous CuO film. *Eur. J. Inorg. Chem.* **2005**, *2005* (23), 4775−4779.
(35) Xie, W. Y.; Song, F.; Wang, X. L.; Wang, Y. Z. Development of Copper Phosphate Nanoflowers on Soy Protein toward a Superhydrophobic and Self-Cleaning Film. *ACS Sustainable Chem. Eng.* **2017**, *5* (1), 869−875.
(36) Kim, D.-H.; Kim, J. Synthesis of LiFePO4 nanoparticles in polyol medium and their electrochemical properties. *Electrochem. Solid-State Lett.* **2006**, *9* (9), A439−A442.
(37) Wang, D.; Buqa, H.; Crouzet, M.; Deghenghi, G.; Drezen, T.; Exnar, I.; Kwon, N.-H.; Miners, J. H.; Poletto, L.; Grätzel, M. High-performance, nano-structured LiMnPO4 synthesized via a polyol method. *J. Power Sources* **2009**, *189* (1), 624−628.
(38) White, M. C.; Decker, A. M.; Chaney, R. L. Metal complexation in xylem fluid: chemical composition of tomato and soybean stem exudate. *Plant Physiol.* **1981**, *67* (2), 292−300.
(39) Elmer, W. H.; DeLaTorre Roche, R.; Pagano, L.; Majumdar, S.; Zuverza-Mena, N.; Dimkpa, C.; Gardea-Torresdey, J.; White, J. Effect of metalloid and metal oxide nanoparticles on Fusarium wilt of watermelon. *Plant Dis.* **2018**, *102*, 1394.
(40) Jeger, M. J.; Viljanen-Rollinson, S. L. H. The use of the area under the disease-progress curve (AUDPC) to assess quantitative disease resistance in crop cultivars. *Theor. Appl. Genet.* **2001**, *102* (1), 32−40.
(41) Lichtenthaler, H. K. [34] Chlorophylls and carotenoids: Pigments of photosynthetic biomembranes. In *Methods in Enzymology*; Yocum, C. F., Ed.; Elsevier, 1987; Vol. *148*, pp 350−382, DOI: 10.1016/0076-6879(87)48036-1.
(42) Hanawalt, J. D.; Rinn, H. W.; Frevel, L. K. Chemical analysis by X-ray diffraction. *Ind. Eng. Chem., Anal. Ed.* **1938**, *10*, 0457−0512.
(43) Langford, J.; Louer, D. High-resolution powder diffraction studies of copper (II) oxide. *J. Appl. Crystallogr.* **1991**, *24* (2), 149−155.
(44) Gao, X.; Avellan, A.; Laughton, S.; Vaidya, R.; Rodrigues, S. M.; Casman, E. A.; Lowry, G. V. CuO Nanoparticle Dissolution and Toxicity to Wheat (Triticum aestivum) in Rhizosphere Soil. *Environ. Sci. Technol.* **2018**, *52* (5), 2888−2897.
(45) Ko, C. K.; Lee, W. G. Effects of pH variation in aqueous solutions on dissolution of copper oxide. *Surf. Interface Anal.* **2010**, *42* (6−7), 1128−1130.
(46) Gunawan, C.; Teoh, W. Y.; Marquis, C. P.; Amal, R. Cytotoxic origin of copper (II) oxide nanoparticles: comparative studies with micron-sized particles, leachate, and metal salts. *ACS Nano* **2011**, *5* (9), 7214−7225.
(47) Fauteux, F.; Remus-Borel, W.; Menzies, J. G.; Belanger, R. R. Silicon and plant disease resistance against pathogenic fungi. *FEMS Microbiol. Lett.* **2005**, *249* (1), 1−6.
(48) Zhao, L.; Hu, Q.; Huang, Y.; Fulton, A. N.; Hannah-Bick, C.; Adeleye, A. S.; Keller, A. A. Activation of antioxidant and detoxification gene expression in cucumber plants exposed to a $Cu(OH)_2$ nanopesticide. *Environ. Sci.: Nano* **2017**, *4* (8), 1750−1760.
(49) Ponmurugan, P.; Manjukarunambika, K.; Elango, V.; Gnanamangai, B. M. Antifungal activity of biosynthesised copper nanoparticles evaluated against red root-rot disease in tea plants. *J. Exp. Nanosci.* **2016**, *11* (13), 1019−1031.

DOI: 10.1021/acssuschemeng.8b03379
ACS Sustainable Chem. Eng. 2018, 6, 14847−14856